Appendix F

Statistical moments of total second order response

The total second order response can be represented in the following two forms:

$$X(t) = \int_{\tau} g_1(\tau)\zeta(t-\tau)d\tau + \int_{\tau_1}\int_{\tau_2} g_2(\tau_1,\tau_2)\zeta(t-\tau_1)\zeta(t-\tau_2)d\tau_1 d\tau_1 \tag{F.1}$$

or

$$= \sum_{i=1}^{\infty}(c_i + \lambda_i W_i)W_i \tag{F.2}$$

From Eq.(F.2) the expected values up to third order are given as follows:

$$E[X] = \sum \lambda_i E[W_i^2] + \sum c_i E[W_i] \tag{F.3}$$

$$E[X^2] = \sum c_i c_j E[W_i W_j] + \sum c_i \lambda_j E[W_i W_j^2] \tag{F.4}$$

$$\begin{aligned} E[X^3] &= \sum c_i c_j c_k E[W_i W_j W_k] + \sum c_i \lambda_j c_k E[W_i W_j^2 W_k] \\ &+ \sum \lambda_i c_j c_k E[W_i^2 W_j W_k] + \sum \lambda_i \lambda_j c_k E[W_i^2 W_j^2 W_k] \\ &+ \sum c_i c_j \lambda_k E[W_i W_j W_k^2] + \sum c_i \lambda_j \lambda_k E[W_i W_j^2 W_k^2] \\ &+ \sum \lambda_i c_j \lambda_k E[W_i^2 W_j W_k^2] + \sum \lambda_i \lambda_j \lambda_k E[W_i^2 W_j^2 W_k^2] \end{aligned} \tag{F.5}$$

Since $W_i (i = 1, \ldots, \infty)$ are the standard Gaussian variables with mutual independence, the following relations[7] are satisfied:

$$E[W_i] = 0 \tag{F.6}$$

$$E[W_i W_j] = \delta_{ij} \tag{F.7}$$

$$E[W_iW_jW_k] = 0 \tag{F.8}$$

$$E[W_iW_jW_kW_l] = \delta_{ij}\delta_{kl} + \delta_{ik}\delta_{jl} + \delta_{il}\delta_{jk} \tag{F.9}$$

$$E[W_iW_jW_kW_lW_m] = 0 \tag{F.10}$$

$$\begin{aligned} E[W_iW_jW_kW_lW_mW_n] &= \delta_{ij}\delta_{kl}\delta_{mn} + \delta_{ij}\delta_{km}\delta_{ln} + \delta_{ij}\delta_{kn}\delta_{lm} \\ &+\delta_{ik}\delta_{jl}\delta_{mn} + \delta_{ik}\delta_{jm}\delta_{ln} + \delta_{ik}\delta_{jn}\delta_{lm} \\ &+\delta_{il}\delta_{jk}\delta_{mn} + \delta_{il}\delta_{jm}\delta_{kn} + \delta_{il}\delta_{jn}\delta_{km} \\ &+\delta_{im}\delta_{jk}\delta_{ln} + \delta_{im}\delta_{jl}\delta_{kn} + \delta_{im}\delta_{jn}\delta_{kl} \\ &+\delta_{in}\delta_{jk}\delta_{lm} + \delta_{in}\delta_{jl}\delta_{km} + \delta_{in}\delta_{jm}\delta_{kl} \end{aligned}$$

$$\text{for } i,j,k,l,m,n = 1,\cdots,\infty \tag{F.11}$$

where δ_{ij} is the Kronecker delta.

Using the above relations, the mean value $\bar{X}$ or $E[X]$, the variance σ_X^2 or $Var[X]$, and the skewness ($\sqrt{\beta_1}$) are obtained as

$$\bar{X} = E[X] = \sum \lambda_i \tag{F.12}$$

$$\sigma_X^2 = Var[X] = E[X^2] - \bar{X}^2 = \sum c_i^2 + 2\sum \lambda_i^2 \tag{F.13}$$

$$\sqrt{\beta_1}\sigma_X^3 = E[X^3] - 3E[X^2]E[X] + 2(E[X])^3 = 8\sum \lambda_i^3 + 6\sum c_i^2\lambda_i \tag{F.14}$$

While from Eq.(F.1) the expected values are written as:

$$E[X] = \int d\tau_1 \int d\tau_2 g_2(\tau_1,\tau_2) R_\zeta(\tau_2-\tau_1) \tag{F.15}$$

$$\begin{aligned} E[X^2] &= \int d\tau_1 \int d\tau_2 g_1(\tau_1) g_1(\tau_2) R_\zeta(\tau_2-\tau_1) \\ &+ \int d\tau_1 \cdots \int d\tau_4 g_2(\tau_1,\tau_2) g_2(\tau_3,\tau_4) \\ &\times [R_\zeta(\tau_2-\tau_1)R_\zeta(\tau_4-\tau_3) + R_\zeta(\tau_2-\tau_3)R_\zeta(\tau_1-\tau_4) \\ &+R_\zeta(\tau_2-\tau_4)R_\zeta(\tau_3-\tau_1)] \end{aligned} \tag{F.16}$$

$$\begin{aligned} E[X^3] &= \int d\tau_1 \cdots \int d\tau_4 g_2(\tau_1,\tau_2) g_1(\tau_3) g_1(\tau_4) \\ &\times [6R_\zeta(\tau_3-\tau_1)R_\zeta(\tau_1-\tau_4) + 3R_\zeta(\tau_2-\tau_1)R_\zeta(\tau_4-\tau_3)] \\ &+[\int d\tau_1 \int d\tau_2 g_2(\tau_1,\tau_2) R_\zeta(\tau_2-\tau_1)]^3 \\ &+ \int d\tau_1 \cdots \int d\tau_6 g_2(\tau_1,\tau_2) g_2(\tau_3,\tau_4) g_2(\tau_5,\tau_6) \\ &\times [6R_\zeta(\tau_2-\tau_1)R_\zeta(\tau_6-\tau_3)R_\zeta(\tau_5-\tau_4) \\ &+8R_\zeta(\tau_3-\tau_1)R_\zeta(\tau_5-\tau_2)R_\zeta(\tau_6-\tau_4)] \end{aligned} \tag{F.17}$$

Transforming Eqs.(F.15), (F.16) and (F.17) to frequency domain we get:

$$\bar{X} = \int d\omega G_2(\omega, -\omega) S_\zeta(\omega) \tag{F.18}$$

$$\sigma_X^2 = \int d\omega |G_1(\omega)|^2 S_\zeta(\omega) + \int d\omega_1 \int d\omega_2 |G_2(\omega_1, \omega_2)|^2 S_\zeta(\omega_1) S_\zeta(\omega_2) \tag{F.19}$$

$$\begin{aligned}\sqrt{\beta_1}\sigma_X^3 &= 6 \int d\omega_1 \int d\omega_2 G_1(-\omega_1) G_1(\omega_2) G_2(\omega_1, \omega_2) S_\zeta(\omega_1) S_\zeta(\omega_2) \\ &+8 \int d\omega_1 \int d\omega_2 \int d\omega_3 G_2(\omega_1, \omega_2) G_2^*(\omega_2, \omega_3) G_2(\omega_3, -\omega_1) \\ &\times S_\zeta(\omega_1) S_\zeta(\omega_2) S_\zeta(\omega_3)\end{aligned} \tag{F.20}$$

where $*$ denotes the complex conjugate.

Cross and Auto spectra

Take the cross correlation function between the nonlinear response process $X(t)$ and the Gaussian wave process $\zeta(t)$ as follows:

$$\begin{aligned}E[(X(t) - \bar{X})\zeta(t-\tau)] &= \int d\tau_1 g_1(\tau_1) E[\zeta(t-\tau_1)\zeta(t-\tau)] \\ &+ \int d\tau_1 \int d\tau_2 g_2(\tau_1, \tau_2) E[\zeta(t-\tau_1) z(t-\tau_2) \zeta(t-\tau)] \\ &- \bar{X} E[\zeta(t-\tau)]\end{aligned} \tag{F.21}$$

Since the wave process is defined to be zero-mean, the last two terms are zero. Thus:

$$E[(X(t) - \bar{X})\zeta(t-\tau)] = \int d\tau_1 g_1(\tau_1) E[\zeta(t-\tau_1)\zeta(t-\tau_1)] \tag{F.22}$$

This means that the cross spectrum involves only the first term in the functional series (F.1), and thus that the linear transfer function G_1 is derivable by standard cross spectrum technique by Fourier transform. Denoting the cross spectrum as $S_{X\zeta}(\omega)$; then we get

$$S_{X\zeta}(\omega) = G_1(\omega) \cdot S_\zeta(\omega) \tag{F.23}$$

Next, taking the auto correlation function of $X(t)$:

$$\begin{aligned}&E[(X(t) - \bar{X})(X(t+\tau) - \bar{X})] \\ &= \int d\tau_1 \int d\tau_2 g_1(\tau_1) g_1(\tau_2) E[\zeta(t-\tau_1)\zeta(t+\tau-\tau_2)]\end{aligned}$$

$$+\int d\tau_1 \cdots \int d\tau_4 g_2(\tau_1,\tau_2)g_2(\tau_3,\tau_4)$$
$$\times E[\zeta(t-\tau_1)\zeta(t-\tau_2)\zeta(t+\tau-\tau_3)\zeta(t+\tau-\tau_4)]$$
$$-\bar{X}^2 \qquad \text{(F.24)}$$

and using the factorization relation[7] for higher order moments of Gaussian processes as:

$$E[X_1X_2X_3X_4] = E[X_1X_2]E[X_3X_4] + E[X_1X_3]E[X_2X_4] + E[X_1X_4]E[X_2X_3] \qquad \text{(F.25)}$$

we obtain

$$\begin{aligned} R_{XX}(\tau) &= \int d\tau_1 \int d\tau_2 g_1(\tau_1)g_1(\tau_2)R_\zeta(\tau+\tau_1-\tau_2) \\ &+ \int d\tau_1 \cdots \int d\tau_4 g_2(\tau_1,\tau_2)g_2(\tau_3,\tau_4) \\ &\times [R_\zeta(\tau+\tau_1-\tau_3)R_\zeta(\tau+\tau_2-\tau_4) \\ &+ R_\zeta(\tau+\tau_1-\tau_4)R_\zeta(\tau+\tau_2-\tau_3)] \end{aligned} \qquad \text{(F.26)}$$

The auto power spectrum is the Fourier transform of R_{XX} and is computed from the Wiener-Khintchine relations as

$$S_X(\omega) = |G_1(\omega)|^2 S_\zeta(\omega) + 2\int d\nu |G_2(\omega-\nu,\nu)|^2 S_\zeta(\omega-\nu)S_\zeta(\nu) \qquad \text{(F.27)}$$

REFFERENCES IN APPENDICES

[1] Ogilvie, T. F. : Second-order hydrodynamic effects on ocean platforms, Proc. International Workshop on Ship and Platform Motions, 1983.

[2] Dalzell, J.F.: Cross-Bi-Spectral Analysis : Application to Ship Resistance in Waves, J.S.R., vol.18, 1974.

[3] Standing, R. G., Dacunha, N. M. C., Matten, R. B.: Mean Wave Drift Forces: Theory and Experiment, NMI R124, 1981.

[4] Watson, G.N.: A Treatise on the Theory of Bessel Functions, Cambridge Univ. Press, 1966.

[5] Kac, M. and Siegert, A.J.F.: On the Theory of Noise in Radio Receiver with Square-Law Detectors, Journ. Appl. Phys., vol.18, 1946.

[6] Courant, R., and Hilbert, D.: Method of Mathematical Physics I, II, Interscience Pub., 1962.

[7] Cramér, H.: Mathematical Method of Statistics, Princeton Unv. Press, 1946.

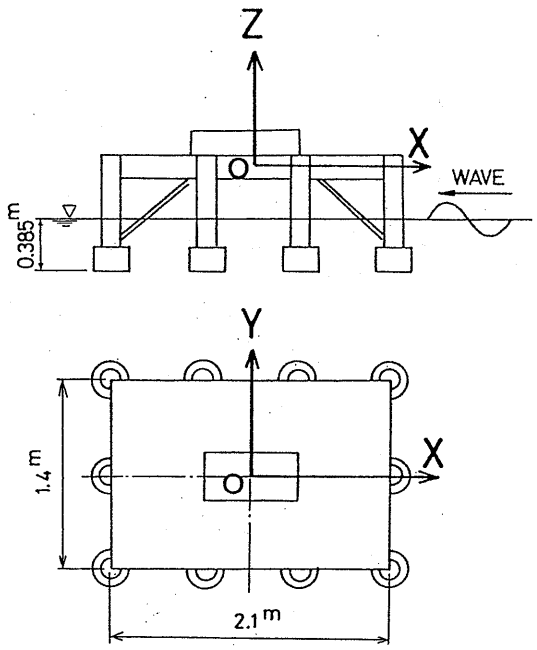

Figure 3.1 Configuration of a floating structure and the direction of incident waves

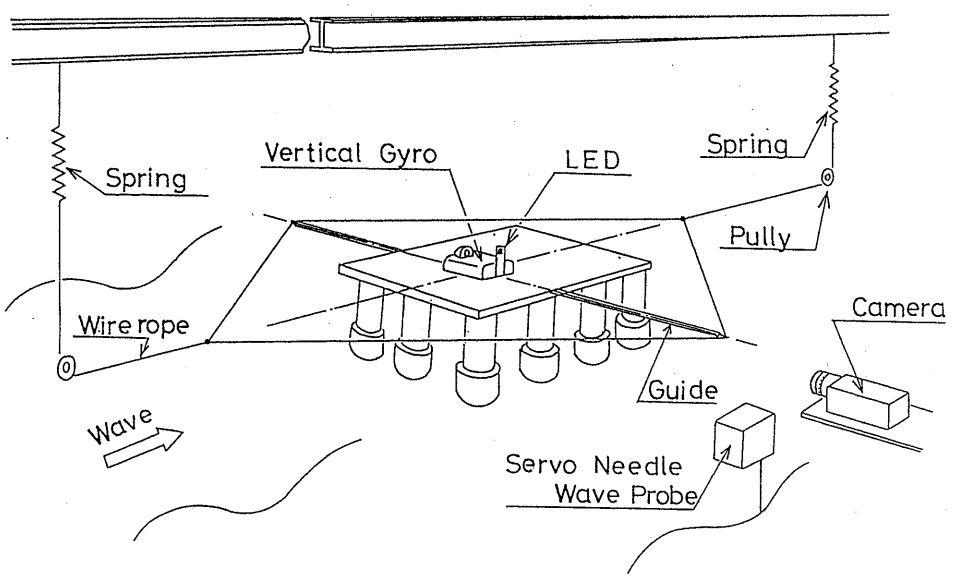

Figure 3.2 Set-up of model test

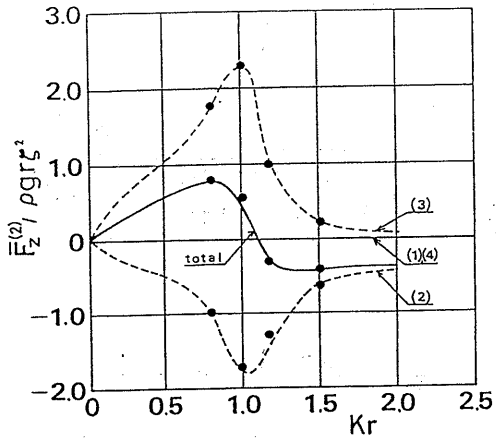

(1) Surface elevation term
(2) Quadratic pressure term
(3) Structure displacement term
(4) Rotation of force vector

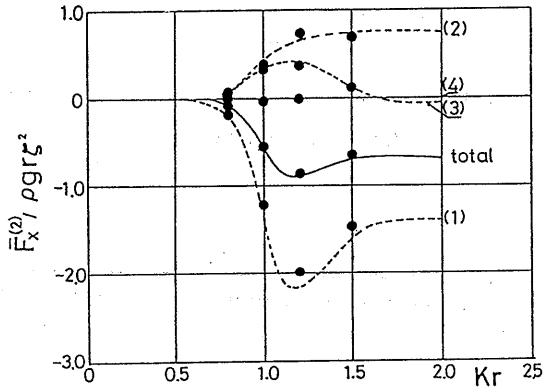

Figure 3.3 Components of the computed mean second order forces of a half sphere

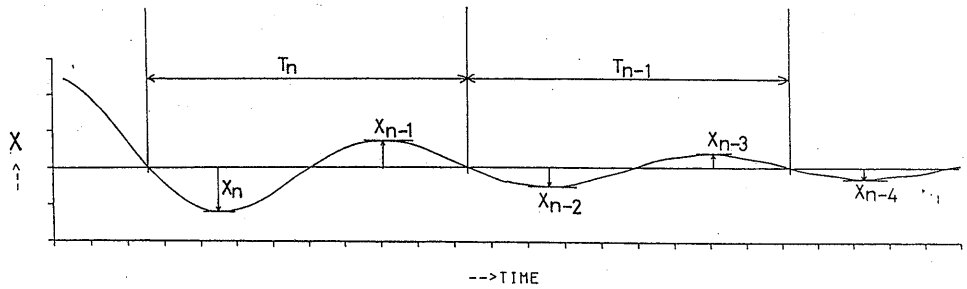

Figure 3.4 An example of the surge decaying motion

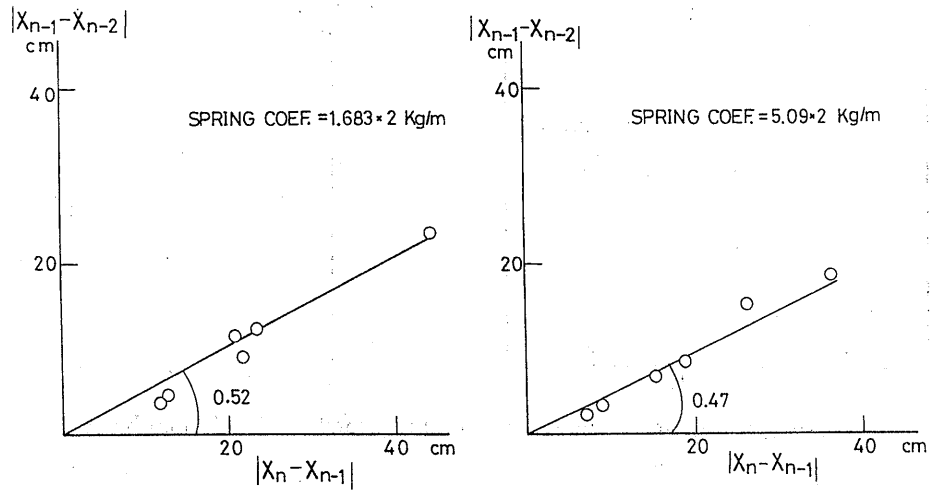

Figure 3.5 Extinction curves of surge motion

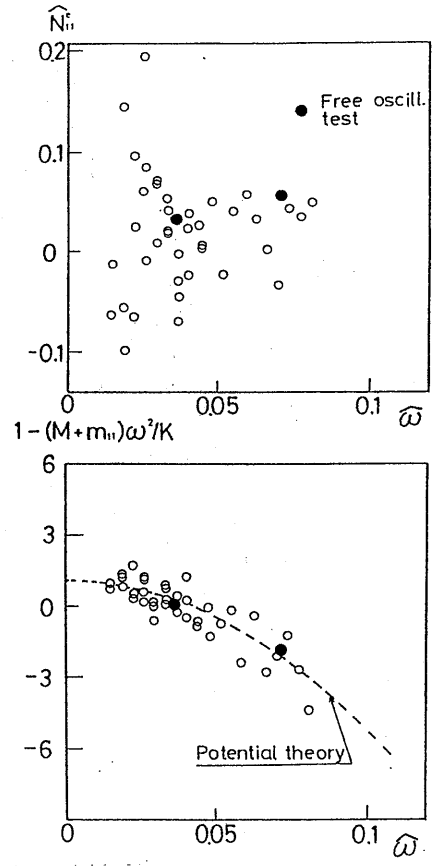

Figure 3.6 Added mass and damping coefficients (frequency base)

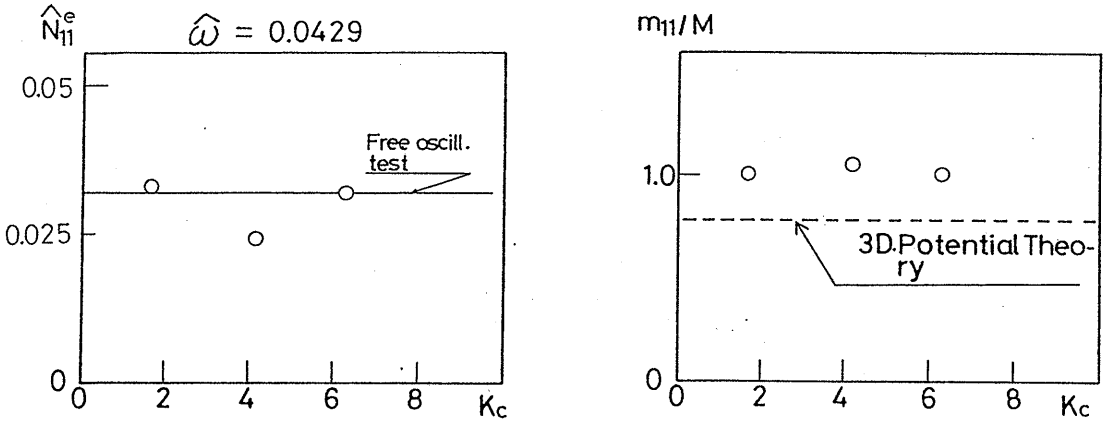

Figure 3.7 Added mass and damping coefficients ($K_c$number base)

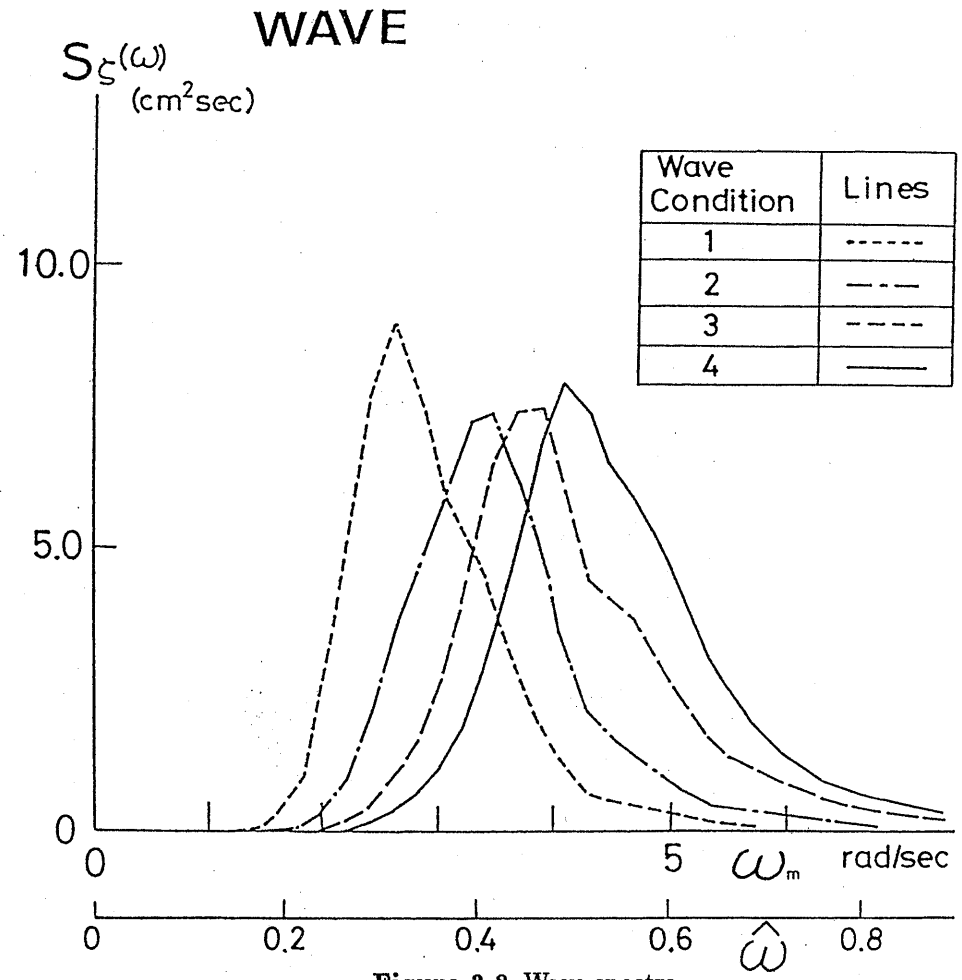

Figure 3.8 Wave spectra

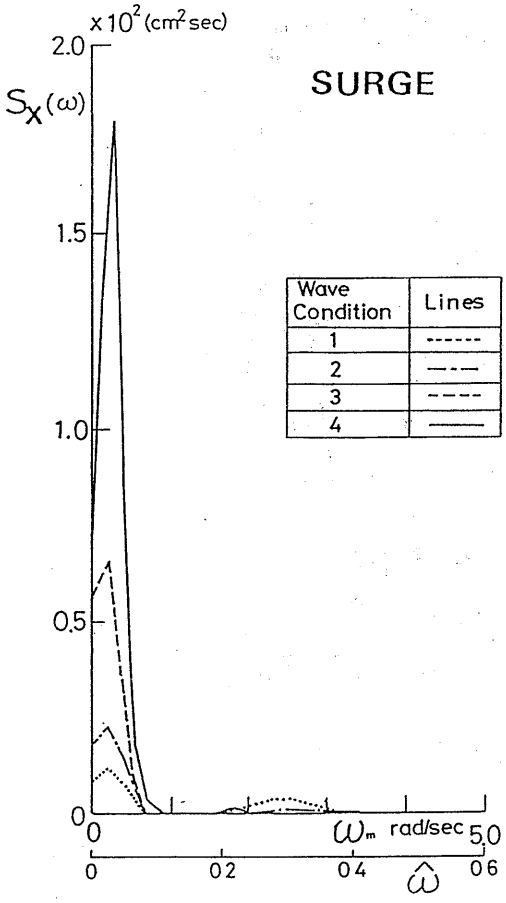

Figure 3.9 Surge response spectra

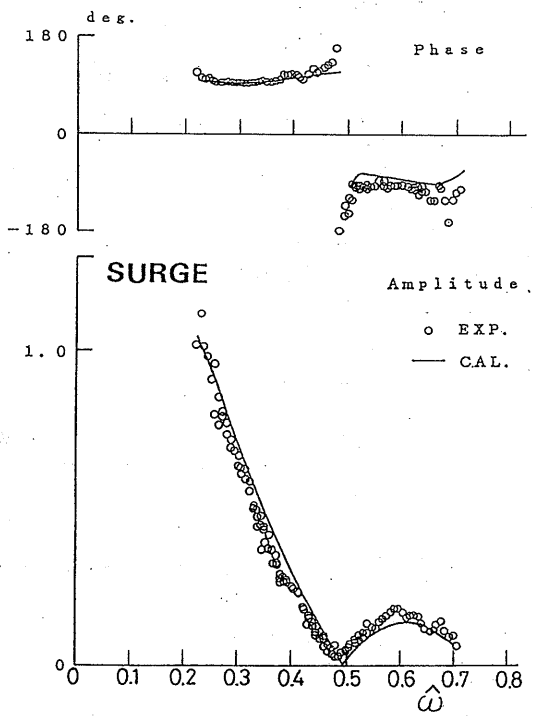

Figure 3.10 Linear transfer function $G_1(\omega)$ of surge motion

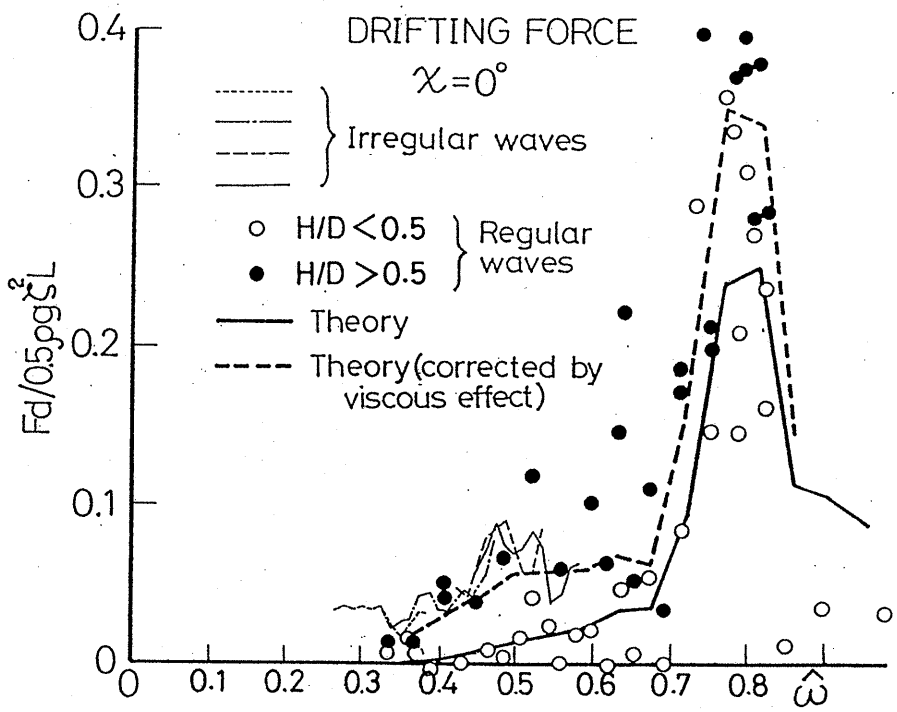

Figure 3.11 Longitudinal steady drift force in head waves

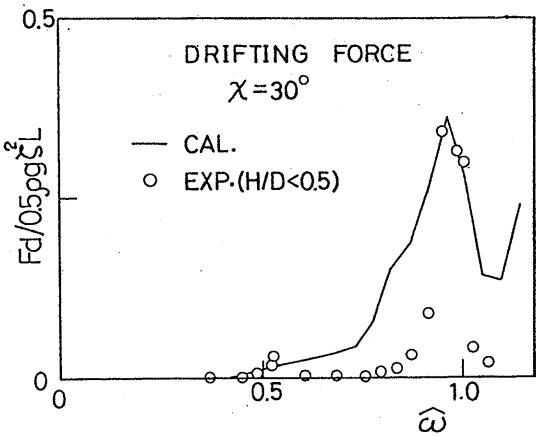

Figure 3.12 Longitudinal steafy drift force in oblique waves ($\chi = 30°$)

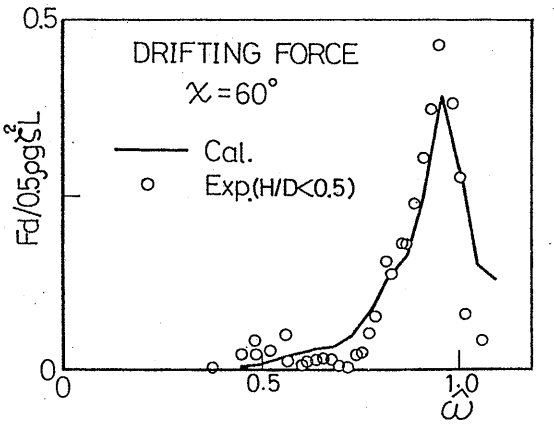

Figure 3.13 Longitudinal steady drift force in oblique waves ($\chi = 60°$)

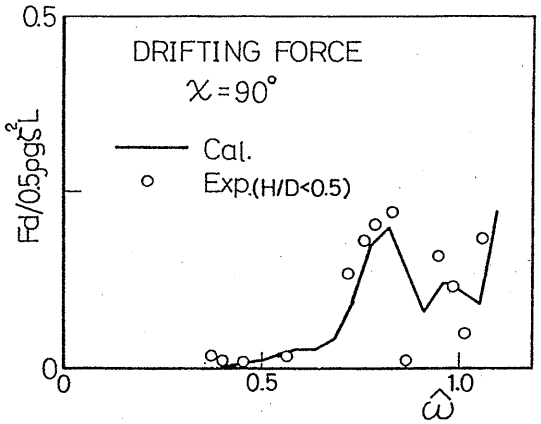

Figure 3.14 Longitudinal steady drift force in beam waves ($\chi = 90°$)

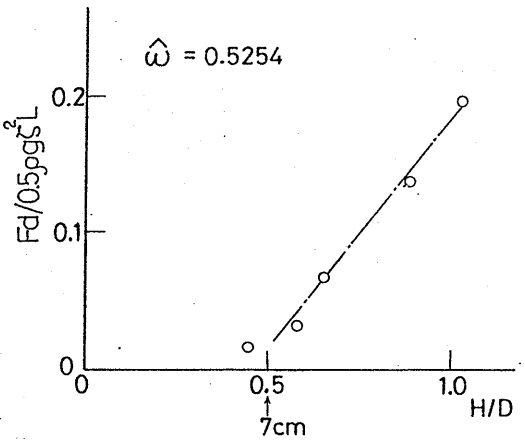

Figure 3.15 a) An example of wave height effect to steady drift force in head waves ($\hat{\omega} = 0.5254$)

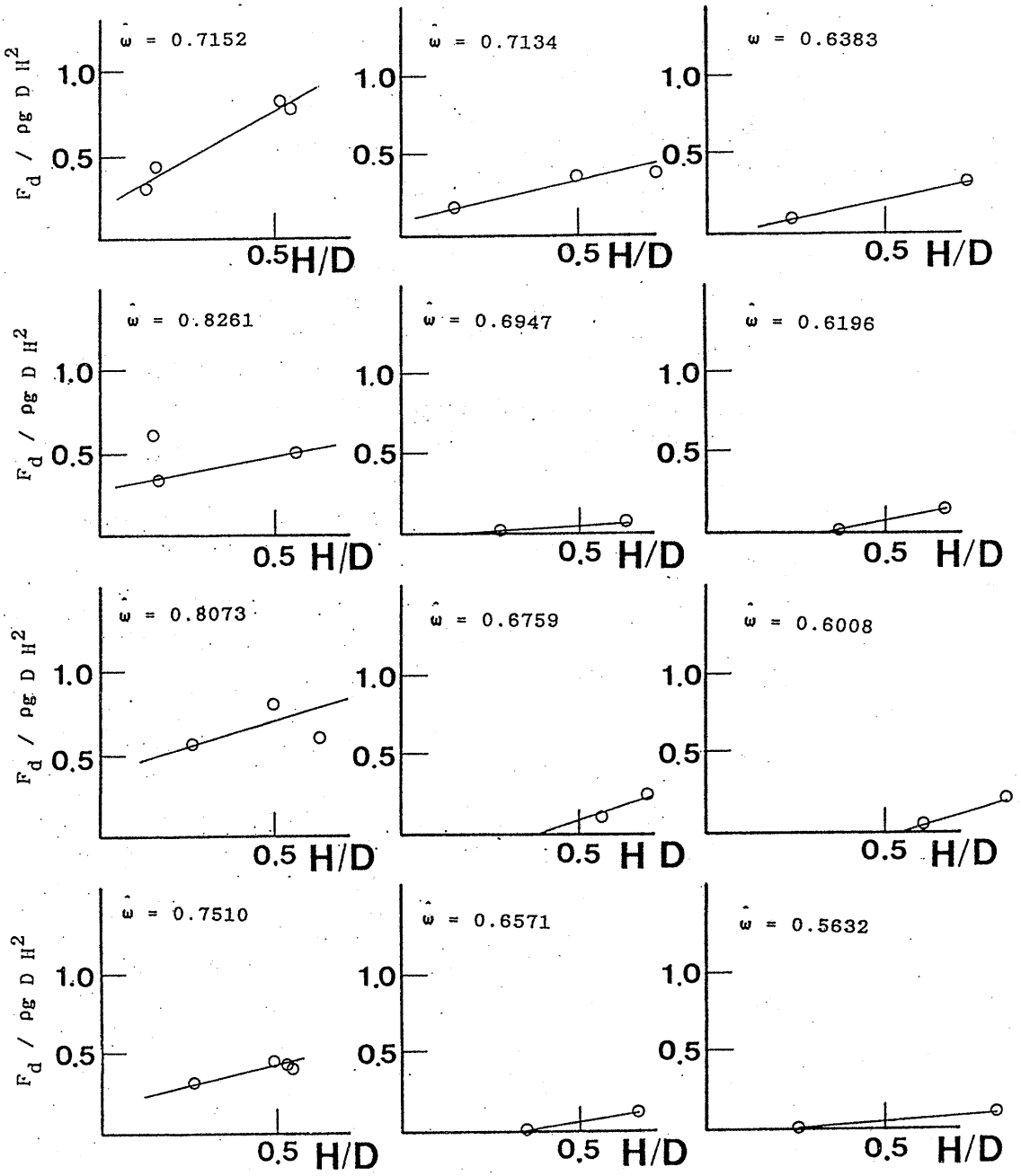

Figure 3.15 b) Wave height effects to steady drift force in head waves

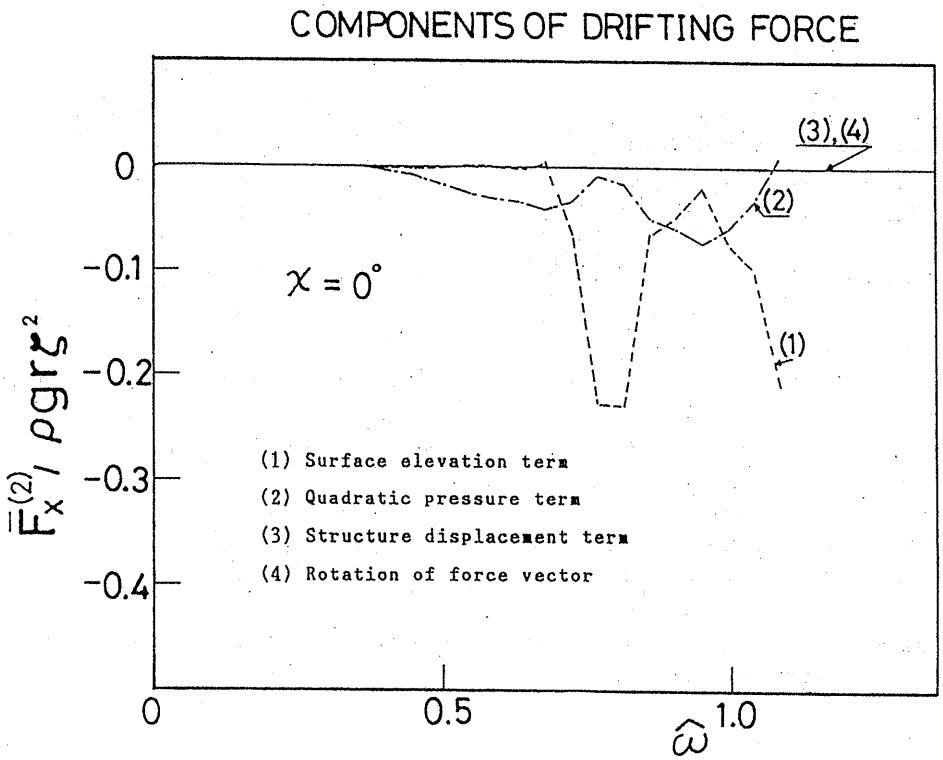

Figure 3.16 Components of steady drift force in head waves where r is half of the length L

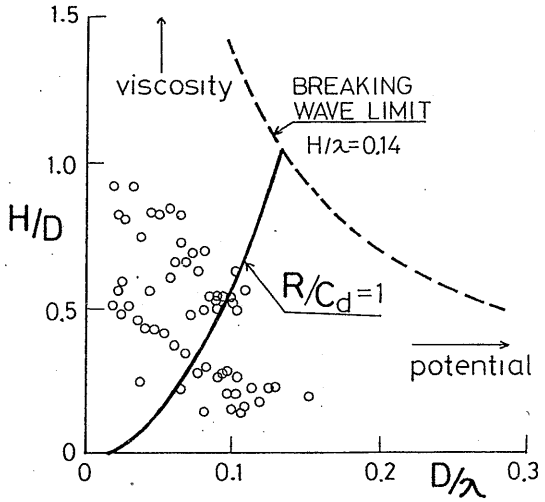

Figure 3.17 Comparison with viscous and potential components of drift forces to a vertical cylinder

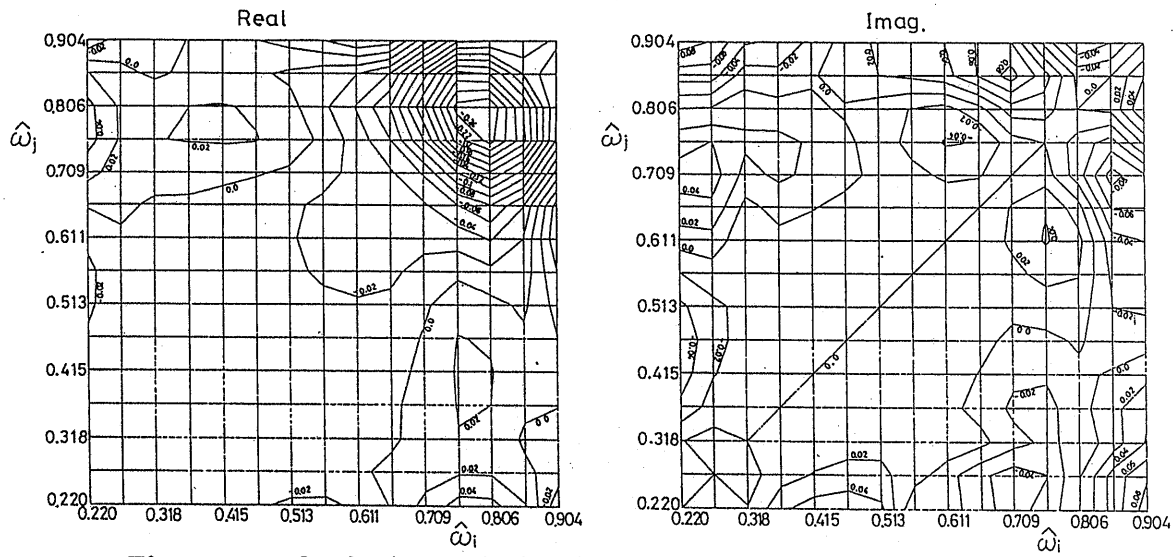

Figure 3.18 Quadratic transfer function of slowly varying drift force obtained from numerical calculation

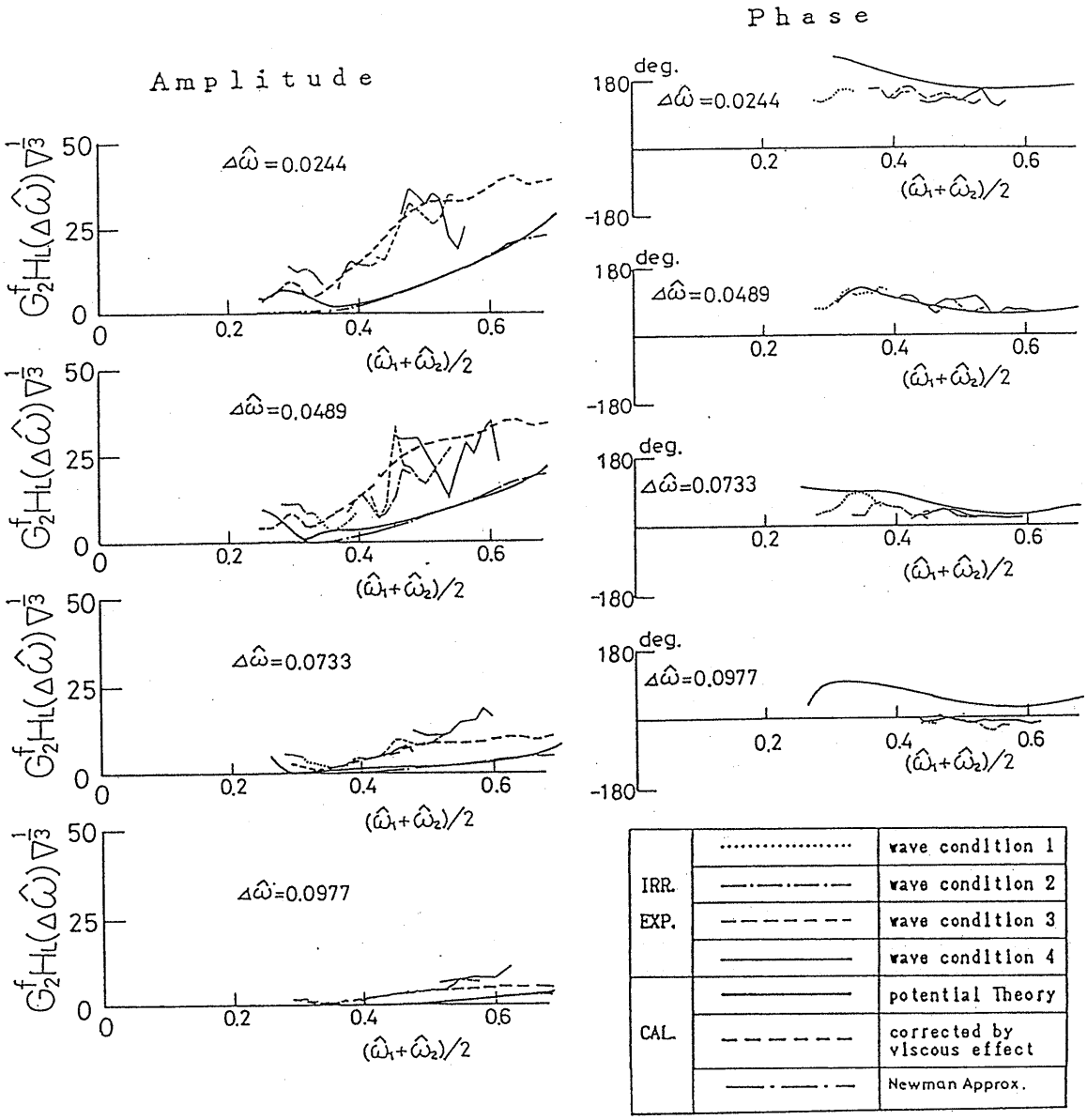

Figure 3.19 Comparison with experimental and numerical results on the quadratic transfer function of slowly varying drift force

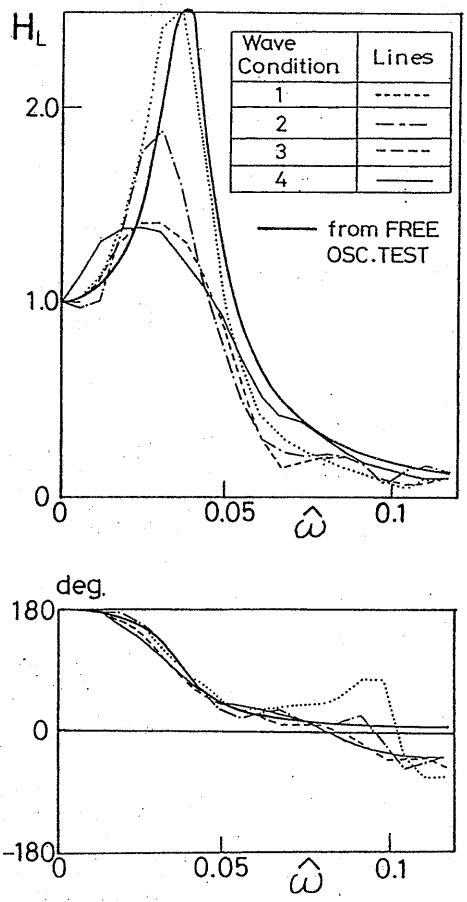

Figure 3.20 Frequency response function $H_L(\omega)$ of surge motion to external forces

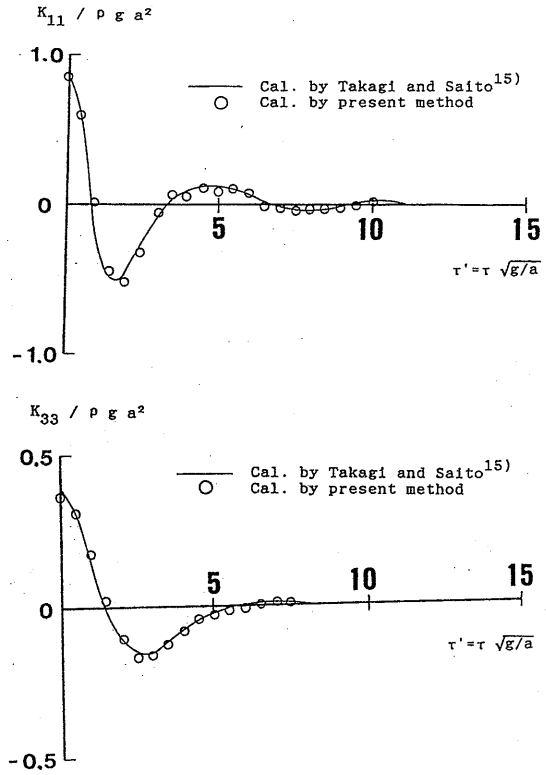

Figure 3.21 Memory effect functions of a half submerged sphere

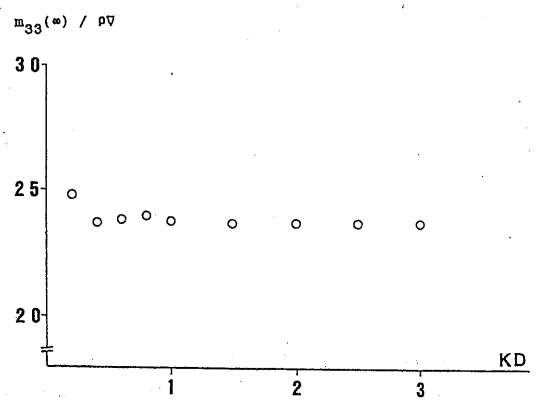

Figure 3.22 Heaving added mass at $\omega = \infty$ of a half submerged rectangular cylinder

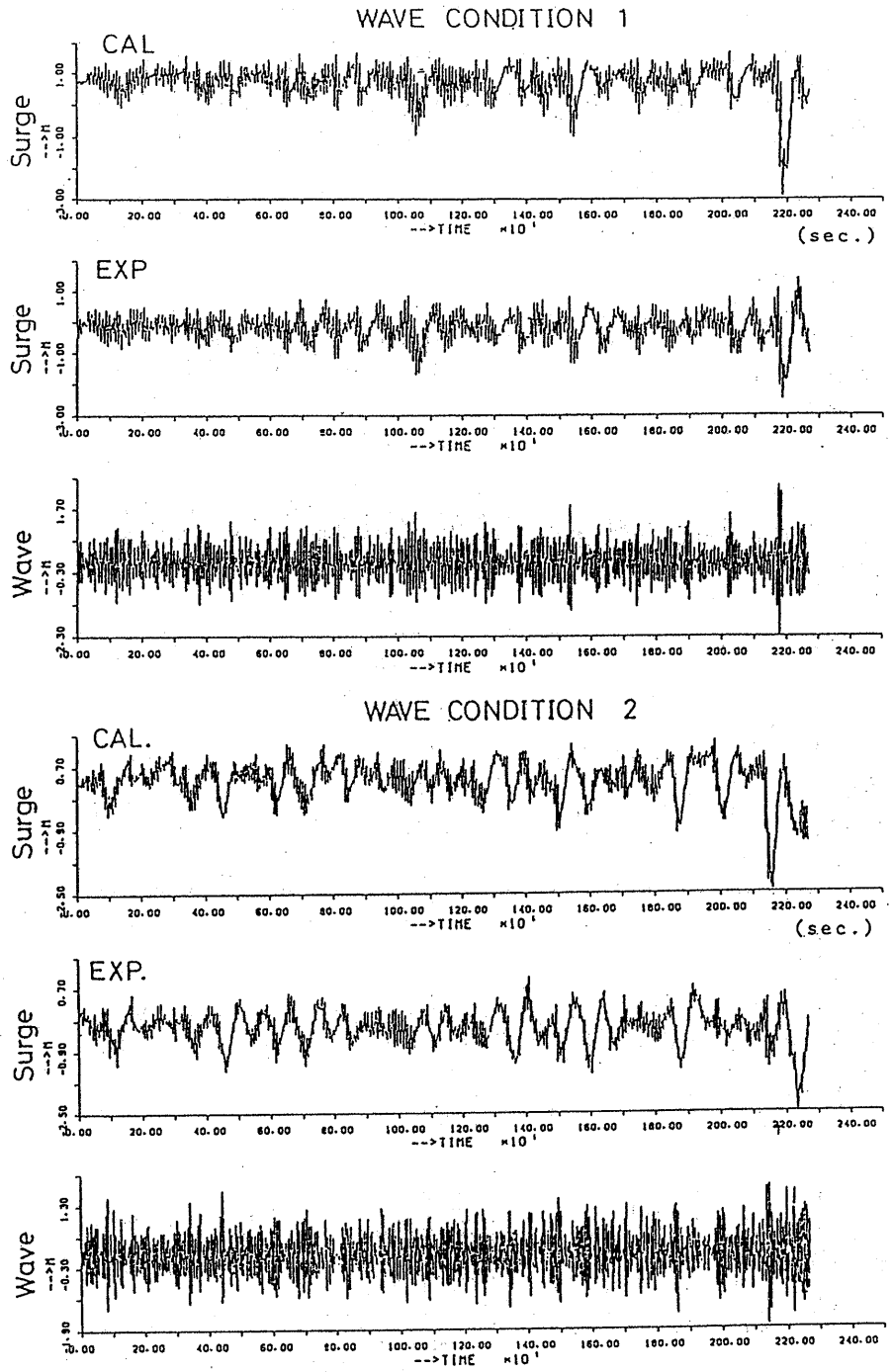

Figure 3.23 Comparisons between surge simulation results and measured ones on the floating body which is moored by linear springs (Wave conditions No1. and No2.)

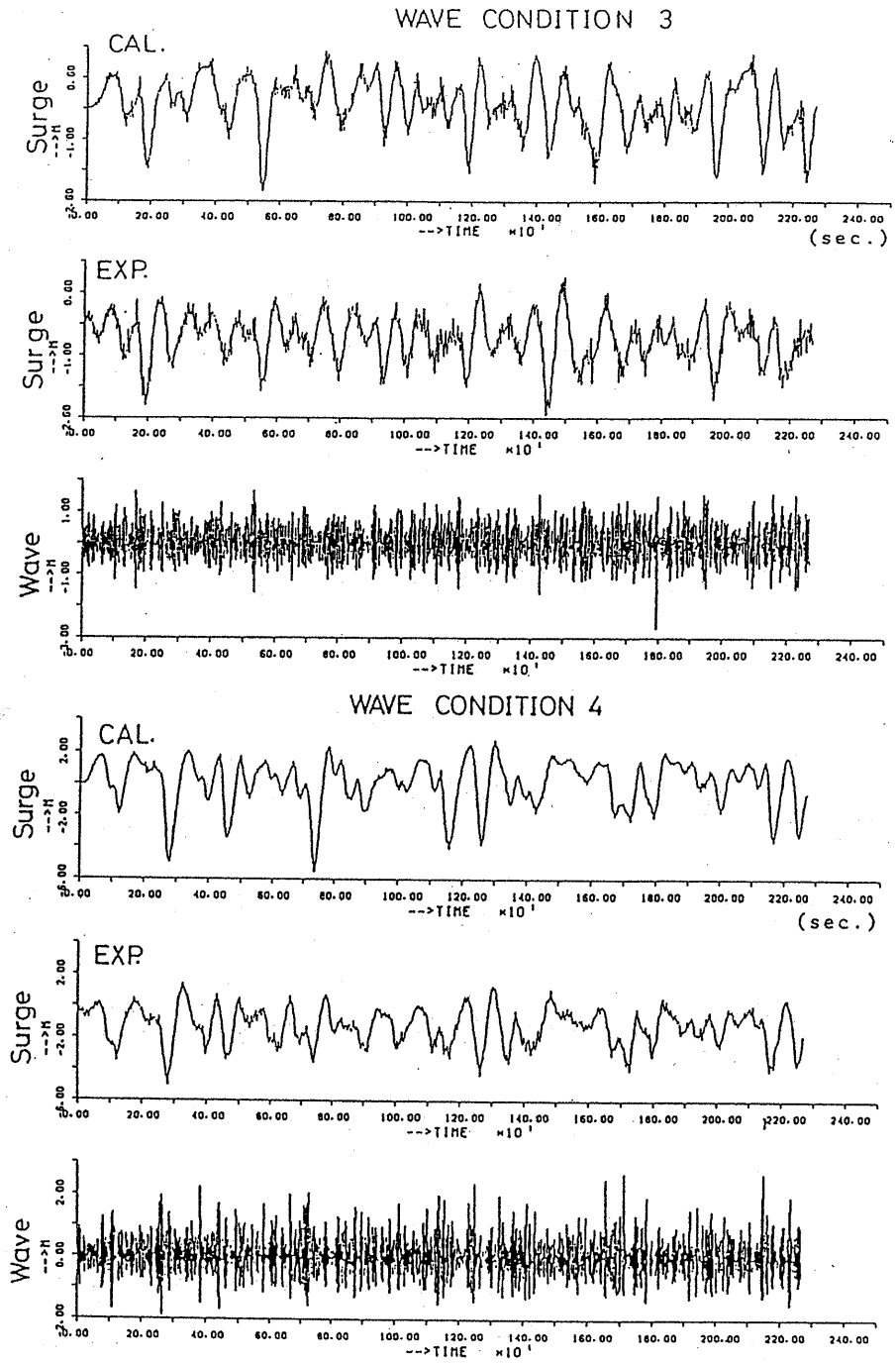

Figure 3.24 Comparisons between surge simulation results and measured ones on the floating body which is moored by linear springs (Wave conditions No3. and No4.)

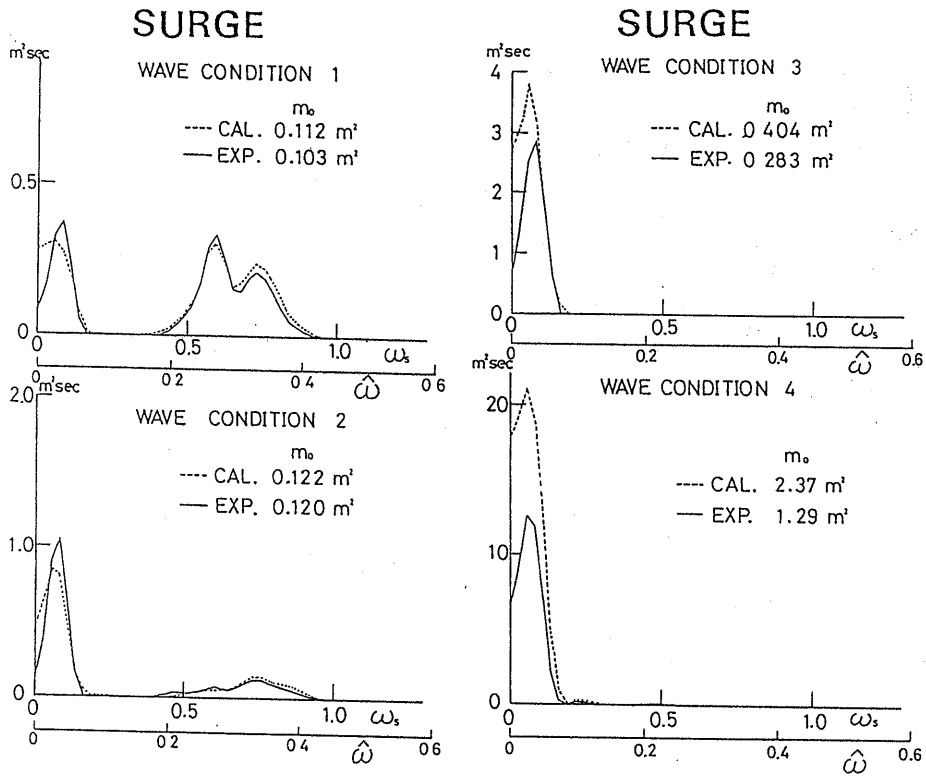

Figure 3.25 Comparisons with surge spectra of simulations and experiments

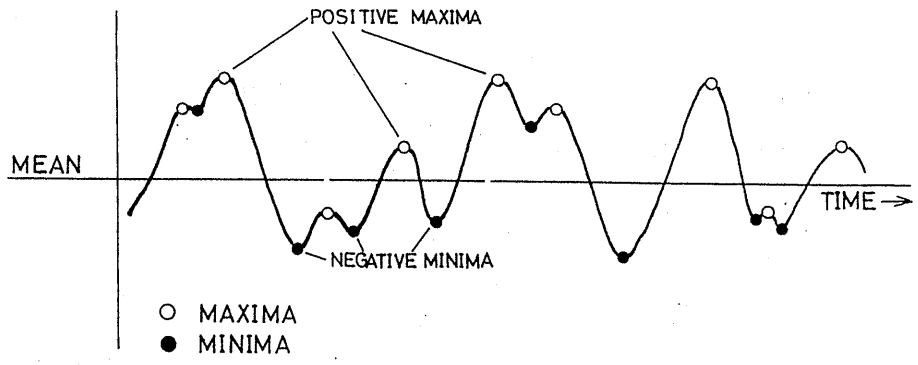

Figure 4.1 Explanatory sketch of a random process $X(t)$

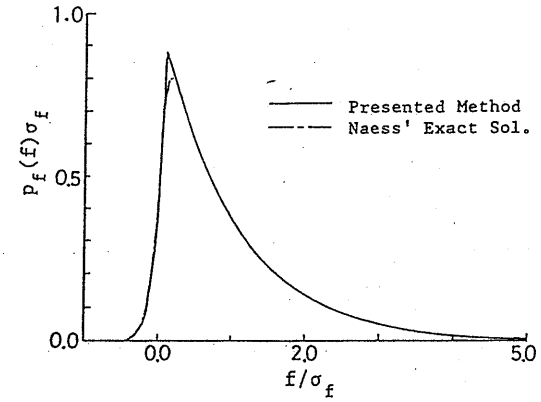

(a) Circular Structure

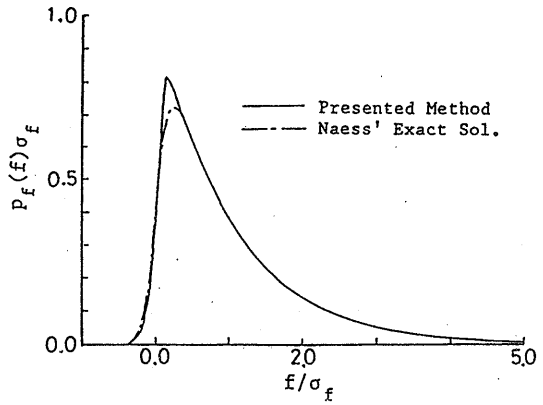

(b) Rectangular Structure

Figure 4.2 Instantaneous p.d.f. of pure second order forces

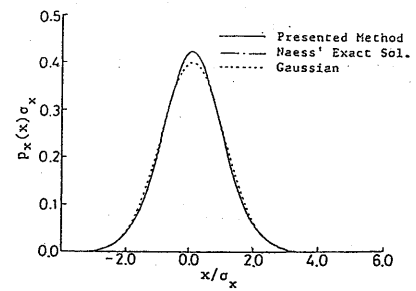

(a) P.D.F. of the Slowly Varying Sway Motion

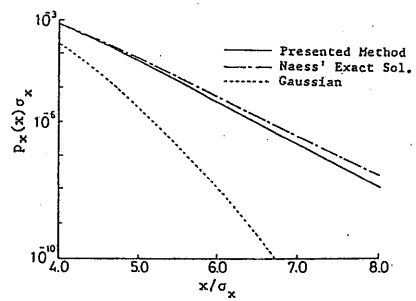

(b) P.D.F. Tail Behaviour

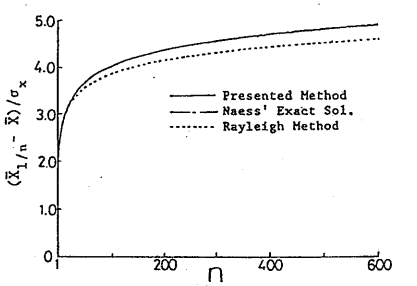

(c) 1/n th Highest Expected Amplitude

Figure 4.3 Instantaneous p.d.f. and 1/n th highest mean amplitude of pure second order responses(Case 1 - circular cylinder)

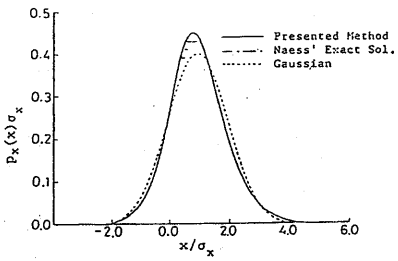

(a) P.D.F. of the Slowly Varying Sway Motion

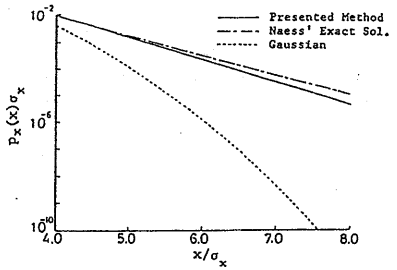

(b) P.D.F. Tail Behaviour

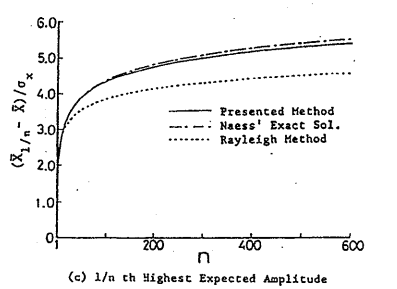

(c) 1/n th Highest Expected Amplitude

Figure 4.4 Instantaneous p.d.f. and 1/n th highest mean amplitude of pure second order responses(Case 2 - circular cylinder)

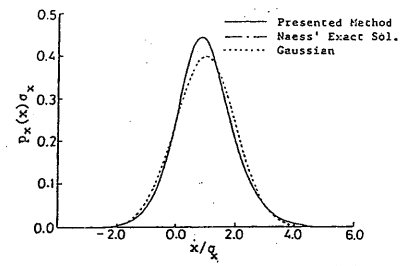

(a) P.D.F. of the Slowly Varying Sway Motion

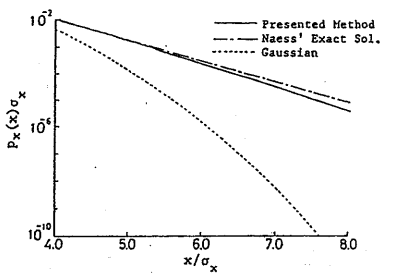

(b) P.D.F. Tail Behaviour

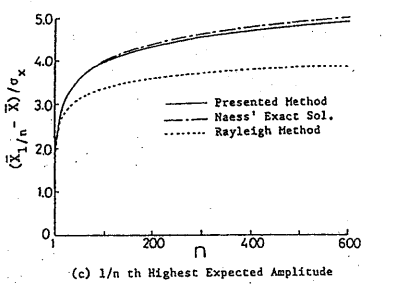

(c) 1/n th Highest Expected Amplitude

Figure 4.5 Instantaneous p.d.f. and 1/n th highest mean amplitude of pure second order responses(Case 3 - rectangular cylinder)

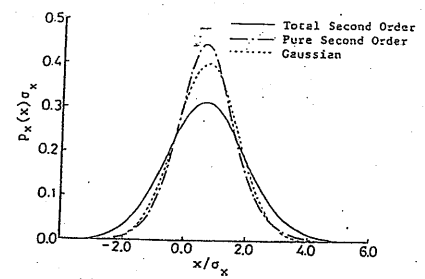

(a) P:D.F. of the Slowly Varying Sway Motion

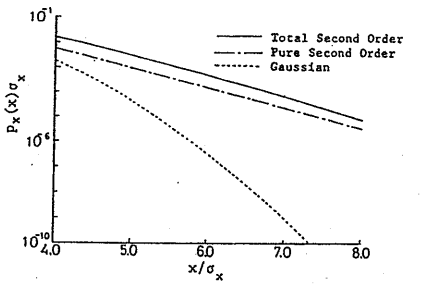

(b) P:D.F. Tail Behaviour

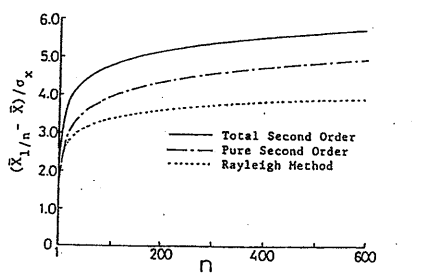

(c) 1/n th Highest Expected Amplitude

Figure 4.6 Statistical interference between first and second order responses for heavy damping($\frac{\sigma_1}{\sigma_2} = 1.36$ and $\kappa = 0.1$)

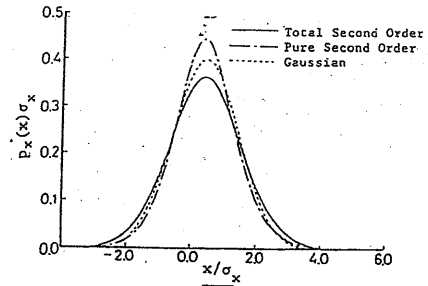

(a) P.D.F. of the Slowly Varying Sway Motion

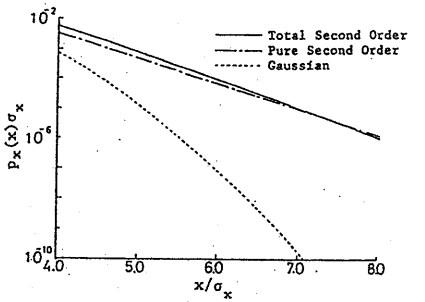

(b) P.D.F. Tail Behaviour

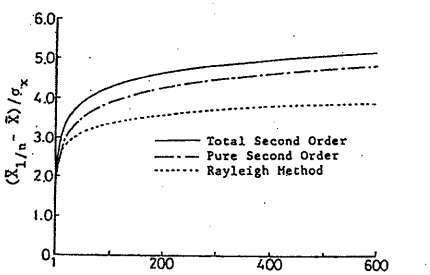

(c) 1/n th Highest Expected Amplitude

Figure 4.7 Statistical interference between first and second order responses for medium damping($\frac{\sigma_1}{\sigma_2} = 2.9$ and $\kappa = 0.006$)

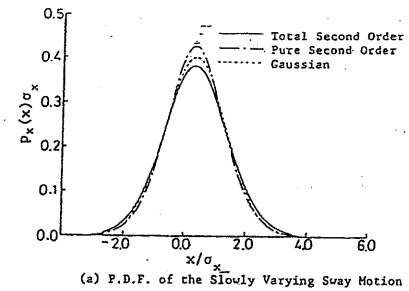

(a) P.D.F. of the Slowly Varying Sway Motion

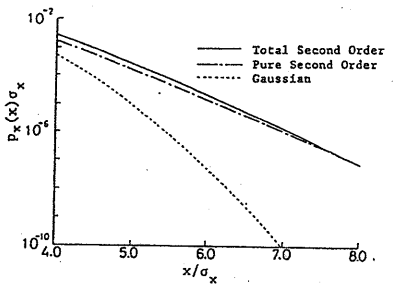

(b) P:D.F. Tail Behaviour

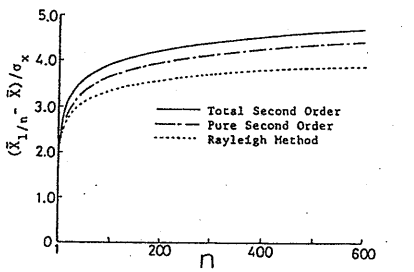

(c) 1/n th Highest Expected Amplitude

Figure 4.8 Statistical interference between first and second order responses for light damping($\frac{\sigma_1}{\sigma_2} = 4.96$ and $\kappa = 0.0001$)

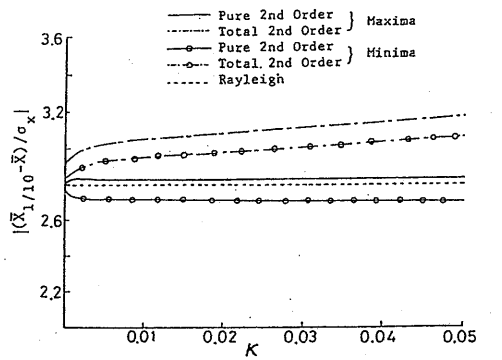

(a) 1/10th Highest Expected Amplitude VS. Damping Coefficient(ω_0=0.1 rad/sec.)

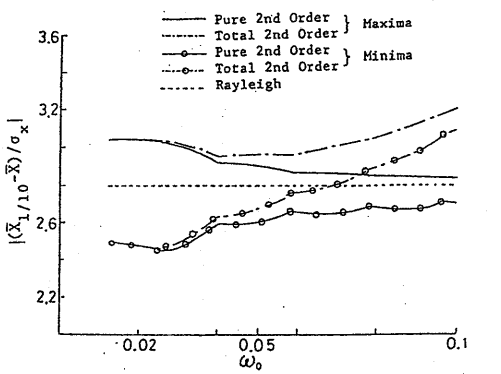

(b) 1/10th Highest Expected Amplitude VS. Natural Frequency(κ=0.06)

Figure 4.9 1/10 th highest mean amplitudes VS. damping coefficient and natural frequency

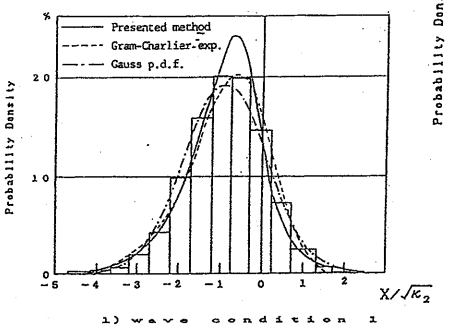

1) wave condition 1

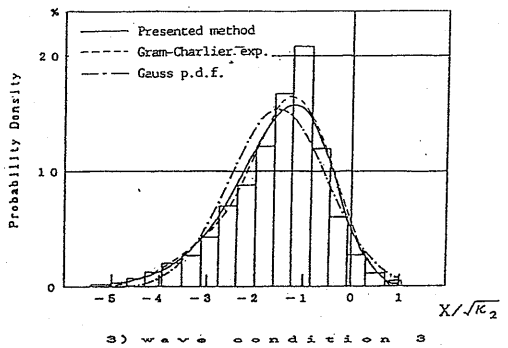

3) wave condition 3

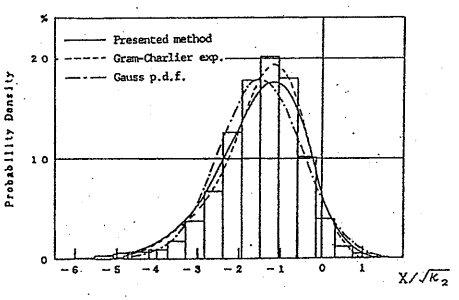

2) wave condition 2

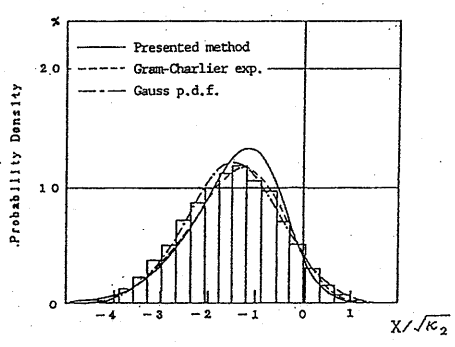

4) wave condition 4

Figure 4.10 Comparisons between observed histograms and estimated instantaneous probability density functions of surge motion (Wave conditions 1 and 2)

Figure 4.11 Comparisons between observed histograms and estimated instantaneous probability density functions of surge motion (Wave conditions 3

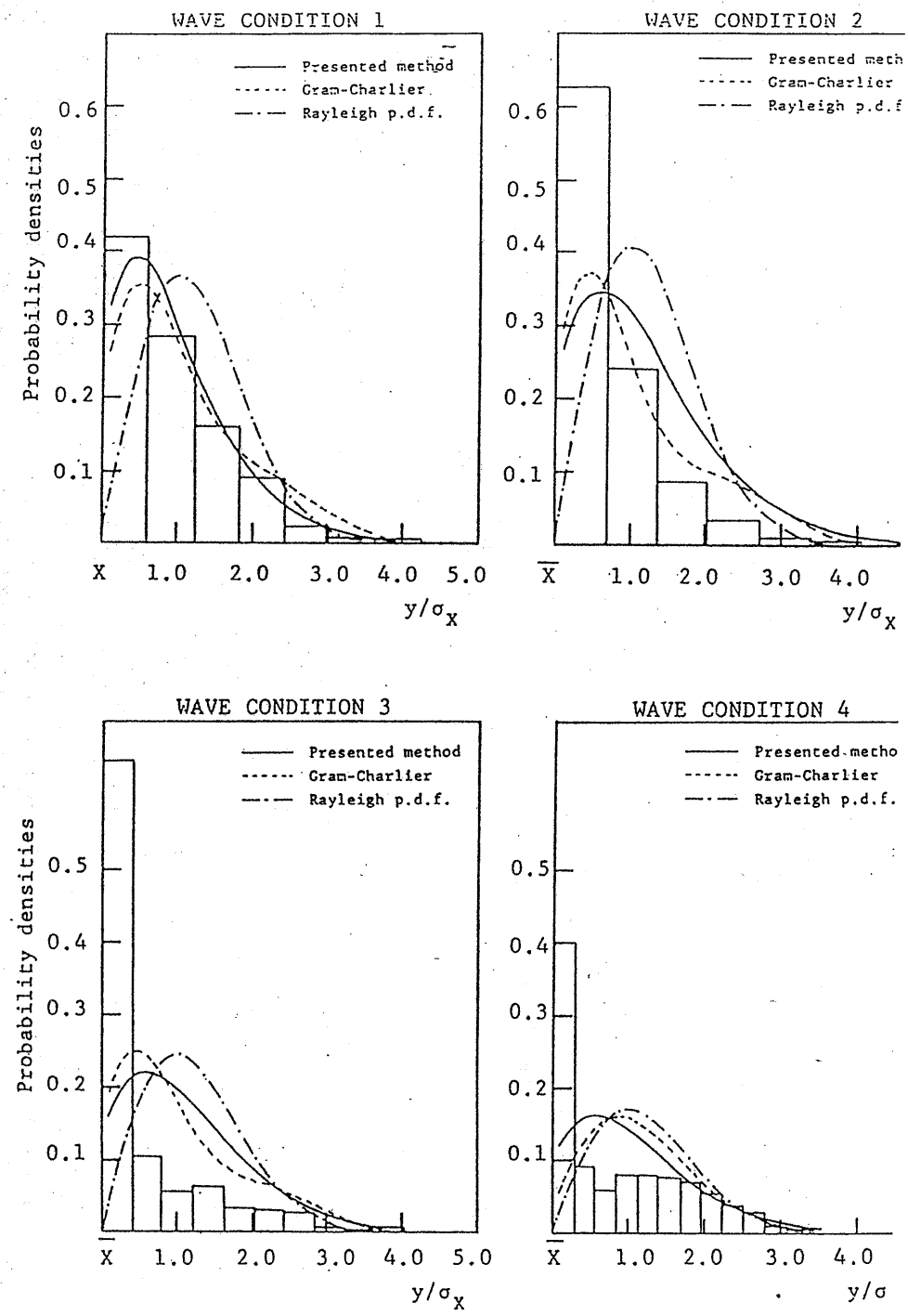

Figure 4.12 Comparisons between observed histograms and estimated maxima probability density functions of surge motion

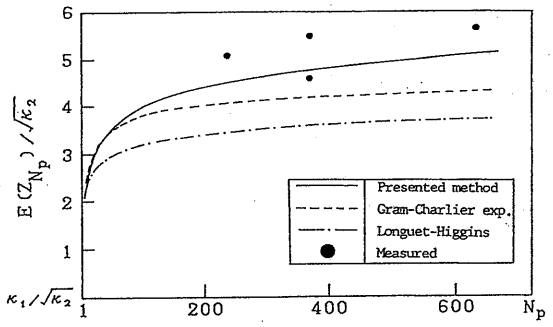

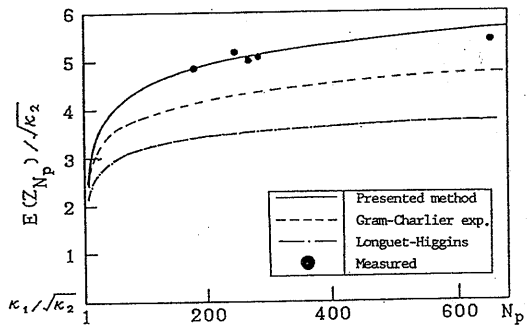

Figure 4.13 Comparisons between observed extreme responses and estimated ones (Wave conditions 1 and 2)

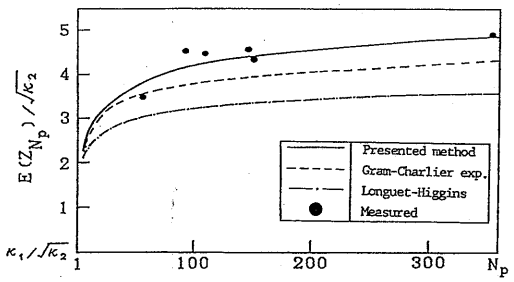

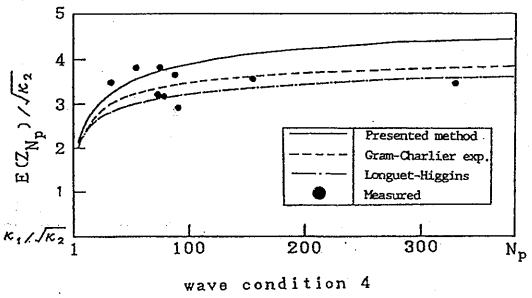

Figure 4.14 Comparisons between observed extreme responses and estimated ones (Wave conditions 3 and 4)

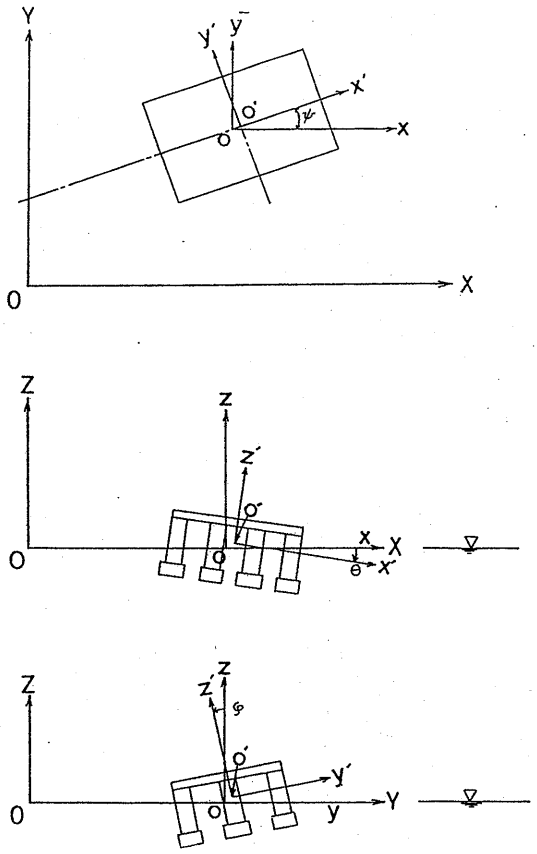

Figure A.1 System of coordinates

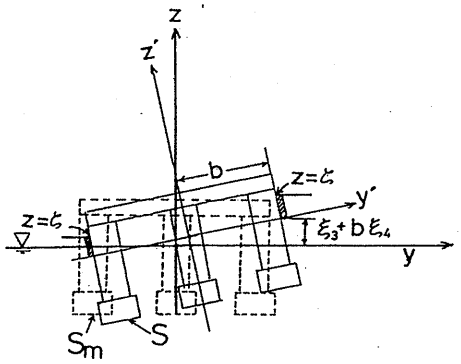

Figure A.2 Relationship between S and S_m

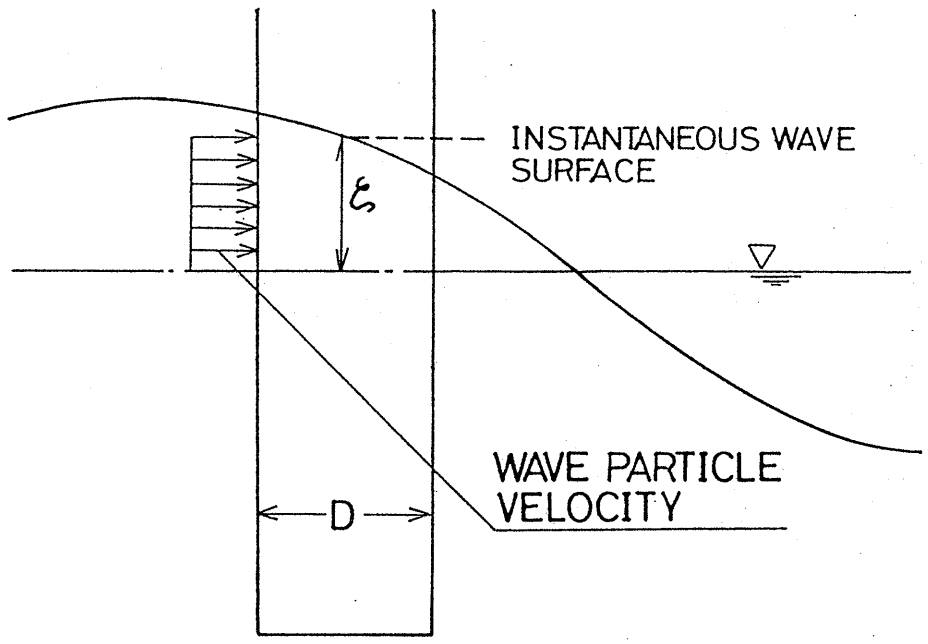

Figure C.1 Contribution to mean force from portion of wave between mean and instantaneous free surface